Abiotic Transformation of Hexahydro-1,3,5-trinito-1,3,5-triazine by Fe II Bound to Magnetite

ARTICLE *in* ENVIRONMENTAL SCIENCE AND TECHNOLOGY · APRIL 2004

Impact Factor: 5.33 · DOI: 10.1021/es034588w · Source: PubMed

4 AUTHORS:

Kelvin B Gregory
Carnegie Mellon University
48 PUBLICATIONS **1,698** CITATIONS
SEE PROFILE

Philip Larese-Casanova
Northeastern University
19 PUBLICATIONS **517** CITATIONS
SEE PROFILE

Gene F Parkin
University of Iowa
71 PUBLICATIONS **2,113** CITATIONS
SEE PROFILE

Michelle Scherer
University of Iowa
83 PUBLICATIONS **4,112** CITATIONS
SEE PROFILE

Environ. Sci. Technol. **2004**, *38,* 1408−1414

Abiotic Transformation of Hexahydro-1,3,5-trinitro-1,3,5-triazine by Fe^{II} Bound to Magnetite

KELVIN B. GREGORY,*,† PHILIP LARESE-CASANOVA, GENE F. PARKIN, AND MICHELLE M. SCHERER

Department of Civil and Environmental Engineering, The University of Iowa, 4105 Seamans Center, Iowa City, Iowa 52242-1527

RDX (hexahydro-1,3,5-trinitro-1,3,5-triazine), a nitramine explosive, is often found as a subsurface contaminant at military installations. Though biological transformations of RDX are often reported, abiotic studies in a defined medium are uncommon. The work reported here was initiated to investigate the transformation of RDX by ferrous iron (Fe^{II}) associated with a mineral surface. RDX is transformed by Fe^{II} in aqueous suspensions of magnetite (Fe_3O_4). Negligible transformation of RDX occurred when it was exposed to Fe^{II} or magnetite alone. The sequential nitroso reduction products (MNX, DNX, and TNX) were observed as intermediates. NH_4^+, N_2O, and HCHO were stable products of the transformation. Experiments with radiolabeled RDX indicate that 90% of the carbon end products remained in solution and that negligible mineralization occurred. Rates of RDX transformation measured for a range of initial Fe^{II} concentrations and solution pH values indicate that greater amounts of adsorbed Fe^{II} result in faster transformation rates. As pH increases, more Fe^{II} adsorbs and k_{obs} increases. The degradation of RDX by Fe^{II}−magnetite suspensions indicates a possible remedial option that could be employed in natural and engineered environments where iron oxides are abundant and ferrous iron is present.

Introduction

Recent military base closures have heightened interest in remediation of sites contaminated with munitions wastes. High-energy explosives such as RDX (hexahydro-1,3,5-trinitro-1,3,5-triazine) form the bulk of munitions contamination, and such compounds will be of growing interest during the dismantling of military arsenals both in the U.S. and abroad (*1*, *2*). Although several ex situ and physical-chemical processes have been developed for RDX removal (e.g., incineration), these methods are costly and not widely accepted by the public. Due to concerns about both the toxicity associated with RDX (*3*, *4*) and its mobility in groundwater (due to high solubility and low tendency to volatilize (*5*)), the cleanup of RDX contamination remains a challenge.

RDX is highly oxidized and therefore susceptible to transformation via reductive processes. Since the first report by McCormick et al. (1981), anaerobic biotransformation has been proposed as a viable strategy for remediation of RDX. Recent studies also suggest that permeable reactive barriers (PRBs) containing zerovalent iron (Fe^0) may be effective for RDX remediation. In the presence of Fe^0 (*6*, *7*) and a mixture of Fe^0 and soil (*6*−*8*), complete removal of RDX from solution has been observed. Rates of RDX transformation were strongly correlated with the amount of Fe^0 initially present. The transformation of RDX in the presence of Fe^0 often results in the production of nitroso intermediates, such as 1,3-dinitro-5-nitroso-1,3,5-triazacyclohexane (MNX), 1,3-dinitroso-5-nitro-1,3,5-triazacyclohexane (DNX), and 1,3,5-trinitroso-1,3,5-triazacyclohexane (TNX). In addition, methylenedinitramine (MEDINA), a ring cleavage product, and NH_4^+, N_2O, and CO_2 have been reported to form from the reaction of RDX with Fe^0.

Although the technology has already been applied at numerous field sites, the importance of understanding the complex mineralogy of Fe^0 barriers has recently become apparent (*9*, *10*). Mineral precipitation in an Fe^0 barrier is influenced by a number of variables including groundwater composition, type of Fe^0 used, target contaminant, and age of the barrier (*10*−*14*). Analysis of laboratory-scale column material and field samples from active barriers has identified a wide array of iron minerals including magnetite, akaganite, mackinawite, lepidocrocite, ferrous sulfide (*15*), goethite (*16*), maghemite (*17*), and green rust (*18*). Mineral precipitates may influence the performance of Fe^0 barriers by acting as a physical barrier, semiconductor, or reactive surface (*19*).

Several of the precipitates observed in Fe^0 barriers contain ferrous iron (Fe^{II}) which can act as a reductant in an oxide lattice or when adsorbed (*20*, *21*). Reactive Fe^{II} precipitates (such as green rust, mackinawite, and magnetite), as well as Fe^{II} adsorbed on oxides, have been shown to reduce a number of environmentally relevant compounds (*22*−*31*) and may form via chemical (*32*, *33*) or microbial reduction (*34*−*38*) of ferric-iron-bearing minerals or clays present in anoxic soils and sediments. The enhanced reactivity of Fe^{II} in the presence of oxide surfaces has been observed in numerous studies with a range of contaminants including, but not limited to, metals (*27*, *28*, *39*), pesticides (*40*, *41*), monochloramine (*31*), nitroaromatic compounds (*25*), and halogenated hydrocarbons (*20*, *29*, *30*). The catalytic activity observed in the presence of oxides and Fe^{II} is thought to be the result of complexation of Fe^{II} with surface hydroxyl groups, similar to that observed for aqueous ligands (*42*−*44*). Fe^{II} is believed to adsorb at the surface and form inner-sphere bonds, which increases the electron density of the adsorbed Fe^{II} (*39*, *45*). In addition, the type of oxide has been shown to affect the catalytic activity. Vikesland and Valentine (*31*) observed the following trend in catalytic activity: magnetite ≫ hematite ≈ lepidocrocite > ferrihydrite for the reduction of monochloramine by Fe^{II}. These results corroborated similar findings with nitroaromatic compounds (*25*) and chromate (*27*). However, in a recent study of oxamyl reduction by 12 different minerals, hematite was found to react faster than goethite (*40*). In this study, the reactivity of Fe^{II} was also found to vary among different suspensions of the same oxide. Variations in the catalytic activity between the different oxides have been attributed to differences in the amount of Fe^{II} adsorbed (*27*), variations in site density (*29*), and differences in Fe surface speciation (due to dissolved metal speciation, type of surface binding, or location of the adsorption site) (*40*).

Field data from a munitions plant in Iowa suggest the RDX reduction does occur in groundwater, but it is unclear

* Corresponding author phone: (413) 545-1048; fax: (413) 545-1578; e-mail: kgregory@microbio.umass.edu.

† Current address: Department of Microbiology, University of Massachusetts, 203 Morrill 4 North, Amherst, MA 01003.

10.1021/es034588w CCC: $27.50
Published on Web 01/21/2004

whether RDX reduction is driven by biological processes or by abiotic reduction mechanisms, such as reduction by structural or adsorbed Fe^{II} species (*46*). Much of the data regarding RDX transformation come from metabolites identified from microbial transformation pathways. To our knowledge, no reports are available regarding the reactivity of RDX with reduced iron species other than Fe^0. We report on an alternative abiotic transformation mechanism for RDX in the presence of Fe^{II} and magnetite (Fe_3O_4). Ferrous iron was added to a suspension of magnetite under various conditions and reacted with RDX. Kinetics studies were performed, as well as product identification for a range of initial Fe^{II} concentrations and solution pH values. Magnetite was selected because it has recently been identified in several PRBs (*14*, *15*) and is commonly found in reduced soils and sediments as a product of biological iron reduction (*34*, *47*, *48*).

Experimental Methods

Chemicals. Aqueous solutions were prepared with ion-exchange, high-purity water (Barnstead NANOpure Diamond), and chemicals were purchased from Sigma-Aldrich Co. Stable carbon and nitrogen isotopes (i.e., [^{12}C]RDX, [^{13}C]RDX, and [^{15}N]RDX) were synthesized according to previously published methods (*49*). The synthesis resulted in a purity of ~98%. [^{14}C]RDX (99.9% purity) was purchased from Perkin-Elmer Life Sciences. Radio-labeled RDX was prepared in an acetone stock solution (0.5 μCi/10 μL). MNX, DNX, and TNX were obtained from SRI International. Stock solutions of RDX and the nitroso derivatives were prepared in acetone and stored at 0 °C. Analytical stock solutions of RDX were purchased from Chem Service, Inc. A stock solution of 0.46 M FerroZine reagent (3-(2-pyridyl)-5,6-bis(4-phenylsulfonic acid)-1,2,4-triazine monosodium salt monohydrate) was prepared in pH 7.0, 50 mM *N*-(2-hydroxyethyl)piperazine-*N*′-2-ethanesulfonic acid (HEPES; $pK_a = 7.5$) buffer and refrigerated. A series of 50 mM buffered solutions were prepared with 2-(*N*-morpholino)ethanesulfonic acid (MES; $pK_a = 6.1$), 3-(*N*-morpholino)propanesulfonic acid (MOPS; $pK_a = 7.2$), and HEPES (*50*, *51*).

Aqueous solutions of Fe^{II} were prepared from anhydrous $FeCl_2$. Fresh stock solutions of ferrous iron (0.4 M) were prepared prior to each experiment in an anaerobic chamber containing 5% H_2:95% N_2 headspace. Stock solutions were filtered through 0.02 μm syringe filters (Anatop 25) from Whatman Scientific prior to use. Magnetite (Fe_3O_4) was purchased from Cerac Inc. The particle size was less than 5 μm, and the mineral phase was determined to be 99% pure on the basis of X-ray diffraction (XRD) patterns provided by Cerac Inc. Magnetite powder was stored at room temperature in the anaerobic chamber. A specific surface area (A, $m^2\ g^{-1}$) of 44 $m^2\ g^{-1}$ was measured under anoxic conditions with N_2 adsorption on a Quantachrome NOVA 1200 Brunauer−Emmett−Teller (BET) surface area analyzer.

RDX Batch Experiments. Unless otherwise noted, all experiments were carried out in an anaerobic chamber (5% H_2:95% N_2) at room temperature and performed in triplicate. The reactors were 125 mL, borosilicate glass serum bottles with aluminum crimps and Teflon-lined butyl rubber septa (Wheaton Science Products, Millville, NJ). Dried magnetite, 0.1 g, was weighed in the anaerobic chamber and added to serum bottles to achieve a surface area concentration of 44 $m^2\ L^{-1}$ in 100 mL. Aliquots of the appropriate organic buffer were added to each bottle and incubated overnight. Aliquots of ferrous stock solution were added from the anoxic stock and allowed to equilibrate for 24 h prior to iron analysis or addition of RDX. Fe^{II} and total iron were measured to ensure that Fe^{II} disappearance was not the result of aqueous oxidation. The 0.02 μm filters were determined to be sufficient for removal of solid magnetite particles (data not shown). Reactors were mixed on a rotary shaker at 40 rpm. Adsorption experiments were initiated by the addition of aliquots of Fe^{II} from stock solutions. Aqueous samples were removed through the septa and filtered through a 0.02 μm syringe filter into 0.5 N HCl for subsequent ferrous iron determinations. RDX transformation experiments were initiated by the addition of aliquots of RDX from an acetone stock solution. Samples were removed through the septa with a syringe and filtered through a 0.02 μm syringe filter into 2 mL, amber, autosampler vials for HPLC analyses. Experiments with [^{14}C]RDX were conducted in 60 mL borosilicate glass serum bottles. Reactors were prepared as described above. Dried magnetite was added to serum bottles to achieve a surface area concentration of 44 $m^2\ L^{-1}$ in 50 mL of 50 mM, pH 7.0 MOPS buffer. Experiments were initiated by addition of the appropriate RDX variant ([^{12}C]RDX, [^{13}C]RDX, [^{14}C]RDX, and [^{15}N]RDX). Each [^{14}C]RDX experiment was spiked to a total radioactivity of approximately 1.8 μCi per reactor. For mineralization experiments, each 60 mL reactor also contained a CO_2 trap consisting of a small test tube with 1.0 mL of 1.0 M NaOH to capture any evolved CO_2. CO_2 traps were incubated on a horizontal shaker at 150 rpm. Initial total radiolabel was determined by filtering 100 μL of sample through a 0.02 μm syringe filter into 20 mL liquid scintillation vials (Research Products International, Inc.) containing 10 mL of Ultima Gold LSC-Cocktail (Packard Biosciences). $^{14}CO_2$ evolution was determined by pouring 1.0 mL of NaOH from the CO_2 trap into 10 mL of LSC-Cocktail.

Chemical Analyses. High-performance liquid chromatography (HPLC) analysis of RDX, MNX, DNX, and TNX was conducted using a Hewlett-Packard 1100 series HPLC instrument equipped with a 250 × 4.6 mm Supelcosil LC-18 column (Supelco, Bellefonte, PA). The mobile phase was isocratic, consisting of deionized water and methanol (4:6, v/v) at a flow rate of 1.0 mL min^{-1}. Detection was spectrophotometric at 240 nm. [^{14}C]RDX and intermediates were quantified by HPLC using a radioactivity detector (Radiomatic, series A-500, Packard Instrument Co., Downers Grove, IL). Total radioactivity and trapped $^{14}CO_2$ were determined by counting on a Beckman LS 6000IC liquid scintillation counter (Beckman Instrument Co., Fullerton, CA)

A Hewlett-Packard model HP5890 gas chromatograph was used to quantify N_2O. Separation was achieved by a GS-Q 0.32 mm i.d., 30 m capillary column (J&W Scientific) using 2 mL min^{-1} of N_2 as carrier gas. The oven temperature was 35 °C, and the detector temperature was 250 °C. The retention time was 1.1 min, and data were collected and integrated using Chemstation Software. Ammonium was measured using a Dionex DX 100 model ion chromatograph. Separation was achieved using a Dionex IonPac CS-12 column with a GS-12 guard column. The eluent was 22 mN H_2SO_4 at a flow rate of 1.0 mL min^{-1}. Data were collected using Chemstation Software.

Analysis for HCHO was performed applying a modified version of EPA method 8315A. Aqueous samples were derivatized with 2,4-dinitrophenylhydrazine (DNPH) in a pH 5.0 acetate buffer agitated at 40 °C for 1 h. The HCHO−DNPH derivative was quantified using a Hewlett-Packard 1100 series HPLC instrument equipped with a 250 × 4.6 mm Supelcosil LC-18 column (Supelco, Bellefonte, PA). The mobile phase was isocratic, consisting of acetonitrile and 13 mM ammonium acetate (4:6, v/v) at a flow rate of 1.0 mL min^{-1}. Detection was spectrophotometric at 360 nm.

Attempts to identify soluble products of RDX transformation were made using liquid chromatography/mass spectrometry (LC/MS) similar to methods employed previously (*8*, *52*, *53*). A Quattro LC (Micromass Corp.) LC/MS/MS equipped with a photodiode array detector was used for soluble RDX intermediates. The mass spectrometer was operated in positive-ion (ES+) and negative-ion (ES−)

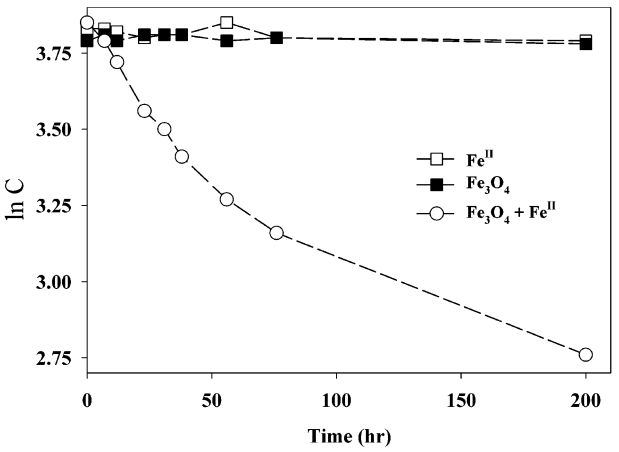

FIGURE 1. First-order plot for transformation of 47 μM RDX in the presence of 1.5 mM initial dissolved Fe^{II} and 44 m^2 L^{-1} magnetite at pH 7.0 (50 mM HEPES buffer).

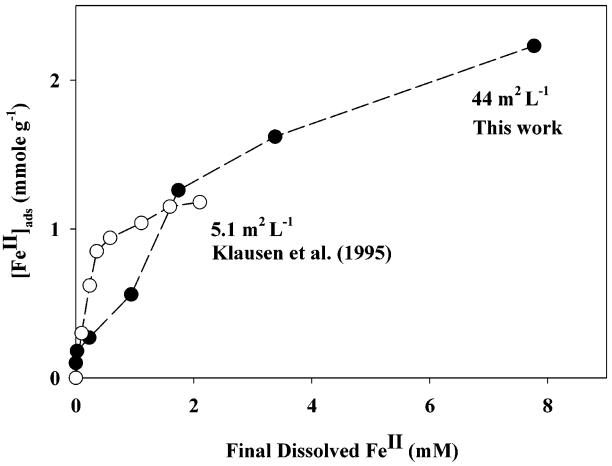

FIGURE 2. Adsorption isotherm for Fe^{II} onto 44 m^2 L^{-1} magnetite in 50 mM, pH 7.0 HEPES buffer.

electrospray modes with desolvation and source temperatures of 150 °C. Analytes were separated using a CN column (Alltech, 25 cm × 4.6 mm, 5 μm) with methanol/water (50:50). Additional separation was attempted using a C-18 column (Supelco, 15 cm × 2.1 mm × 5 mm) with methanol/2 mM ammonium acetate (ES−) or methanol/2 mM acetic acid (ES+). Scanning conditions for the MS were set for masses between 70 and 285 in scanning windows of 5.

Ferrous iron was determined photometrically after complexation with FerroZine (*54*). The method followed for ferrous and total iron (sum of ferrous and ferric) was described by Lovley et al. (*55*). The adsorbed Fe^{II} concentration was estimated by the difference between the initial dissolved ferrous iron concentration $[Fe^{II}]_{dis}$ and the final $[Fe^{II}]_{dis}$ concentration. The final $[Fe^{II}]_{dis}$ was determined again, after 48 h, to check for equilibrium conditions.

Results and Discussion

RDX Transformation by Fe^{II} Bound to Magnetite. RDX was removed in the presence of Fe^{II} and magnetite in pH 7.0 HEPES buffer (Figure 1). No RDX transformation was observed in the presence of magnetite alone at pH 6.0, 6.5, 7.0, 7.5, and 8.0 after a week of exposure. Previous studies have also found that magnetite alone results in negligible reduction of nitroaromatic compounds (*25*). In the absence of magnetite, negligible removal of RDX was observed in the presence of 1.5 mM dissolved Fe^{II} (added as $FeCl_2$) at pH 6.0, 6.5, 7.0, and 7.5 over the time course of these experiments (data not shown). At pH 8.0, however, addition of 1.5 mM Fe^{II} resulted in the formation of a brown precipitate and subsequent removal of 72 μM of RDX over 10 days (data not shown). Heightened reactivity of Fe^{II} in the presence of oxide surfaces has been noted previously (*20*, *25*, *27*−*31*, *39*−*41*). It is thought that the accelerated rates in the presence of oxides is the result of complexation of Fe^{II} with surface hydroxyl groups, similar to that observed with aqueous ligands (*42*−*44*, *56*).

Under the conditions of the experiments shown in Figure 1 (pH 7.0 and $[Fe^{II}]_{ads}$ = 0.27 mmol g^{-1}), the rate of RDX transformation became slower as time progressed. A similar trend has been observed previously for nitroaromatic and pertechnetate reduction by adsorbed Fe^{II} (*25*, *29*). The deviation from first-order kinetics observed in this experiment is expected as the number of electrons available from the Fe^{II} adsorbed (about 27 μmol assuming one electron available per Fe^{II}) is similar to the number of electrons required to reduce RDX to TNX (about 28 μmol) and much less than the number required to reduce the nitro groups to NH_4^+ as final products. Presumably, as time progresses, the Fe^{II} becomes depleted and insufficient reductant is available, resulting in the observed deviation from first-order kinetics.

Effect of Fe^{II} Concentration on Fe^{II} Adsorption and RDX Transformation Rates. To explore variations in rates as a function of the amount of adsorbed Fe^{II}, we measured rates of RDX transformation for a range of initial Fe^{II} concentrations and solution pH values. As the concentration of initial dissolved Fe^{II} ($[Fe^{II}]_{dis}$) was increased from 0.1 to 10.0 mM in pH 7.0 HEPES buffer, more Fe^{II} adsorbed onto magnetite (Figure 2). More adsorption at higher initial Fe^{II} concentration is consistent with what others have reported for adsorption of Fe^{II} onto a variety of iron oxides (*29*, *30*, *40*, *57*), including magnetite (*25*).

Data reported by Klausen et al. (1995) (*25*) are plotted in Figure 2 for comparison with our data. Although the trends are similar at low dissolved Fe^{II} concentrations, we did not observe the plateau behavior indicative of site saturation until much higher initial concentrations of Fe^{II}. One explanation may be that our experiments contained almost a 10-fold higher surface area concentration of magnetite compared to those of Klausen et al. (44 m^2 L^{-1} compared to 5.1 m^2 L^{-1}). Alternatively, the observation of Fe^{II} sorption increasing with higher Fe^{II} concentrations on both goethite and hematite has been interpreted as a transition from surface complexation to surface precipitation or formation of a solid−solution (*30*, *58*, *59*). Our understanding of the nature of the Fe^{II} interaction with the Fe^{III} oxide surface is limited, however, by our inability to directly observe Fe adsorbed at the iron oxide−water interface. Advances in the application of spectroscopic technique, such as grazing-incidence X-ray absorption spectroscopy or Mössbauer spectroscopy, may provide a way to overcome this limitation (*60*).

Rates of RDX transformation increase as the amount of Fe^{II} adsorbed increases (Figure 3). At low concentrations of adsorbed Fe^{II} (<0.18 mmol g^{-1}), little transformation of RDX is observed. At higher concentrations (>0.27 mmol g^{-1}), RDX is completely removed within about 3 days and the kinetics appear first-order over the full time course of the experiment. It is interesting to note that, at the two lower concentrations (where negligible RDX transformation occurred), there was little Fe^{II} in solution available to regenerate the surface (Table 1). Similar observations led others (*25*) to suggest that regeneration of adsorbed Fe^{II} might be the rate-limiting step in the reduction of nitroaromatic compounds by Fe^{II} adsorbed to magnetite. Recent work with carbon tetrachloride found that regeneration of the adsorbed Fe^{II} (from solution) was necessary to balance the number of electrons needed to account for the observed carbon tetrachloride reduction and maintain pseudo-first-order kinetics (*29*). Our results support

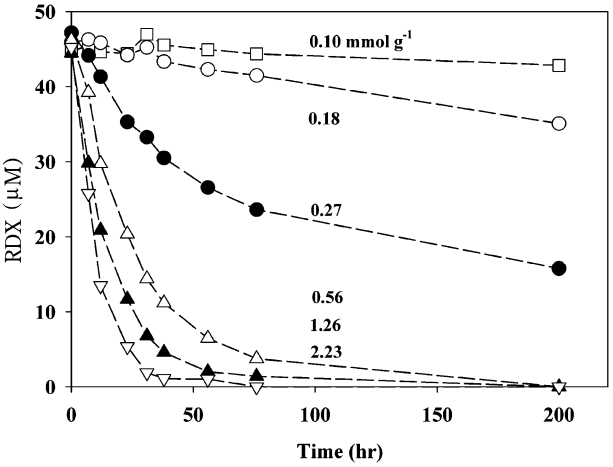

FIGURE 3. Transformation of RDX by various concentrations of Fe^{II} on 44 m^2 L^{-1} magnetite.

TABLE 1. Data for Fe^{II} Adsorption onto Magnetite and k_{obs} Measured for the Transformation of 50 μM RDX[a]

pH	buffer	initial $[Fe^{II}]_{dis}$ (mM)	final $[Fe^{II}]_{dis}$ (mM)	$[Fe^{II}]_{ads}$[b] (mmol g^{-1})	k_{obs}[d,e] (h^{-1})
			Varying $[Fe^{II}]$		
7.0	HEPES	0.00	0.00	0.00	ND[c]
7.0	HEPES	0.10	0.00	0.10	3.0×10^{-4}
7.0	HEPES	0.20	0.02	0.18	1.4×10^{-3}
7.0	HEPES	0.50	0.23	0.27	1.2×10^{-2}
7.0	HEPES	1.50	0.94	0.56	3.6×10^{-2}
7.0	HEPES	3.00	1.74	1.26	6.0×10^{-2}
7.0	HEPES	5.00	3.38	1.62	7.4×10^{-2}
7.0	HEPES	10.00	7.77	2.23	1.0×10^{-1}
			Varying pH		
6.0	MES	1.60	1.42	0.16	$(2.2 \pm 0.1) \times 10^{-3}$
6.5	MOPS	1.60	1.34	0.24	$(1.7 \pm 0.3) \times 10^{-2}$
7.0	MOPS	1.60	1.21	0.37	$(5.9 \pm 0.6) \times 10^{-2}$
7.0	HEPES	1.60	1.01	0.57	$(6.6 \pm 0.4) \times 10^{-2}$
7.5	HEPES	1.60	0.76	0.82	$(3.2 \pm 0.8) \times 10^{-1}$
8.0	HEPES	1.60	0.56	1.01	$(2.6 \pm 0.1) \times 10^{-1}$

[a] 44 m^2 L^{-1} magnetite, 50 mM buffer. [b] Estimated from initial $[Fe^{II}]_{dis}$ − final $[Fe^{II}]_{dis}$. [c] No detectable change in RDX concentration was observed over 200 h. [d] Standard deviations given on the basis of triplicate reactors. [e] Determined from the slope of ln *C* versus time using initial points.

the hypothesis that sufficient Fe^{II} is needed in solution to support appreciable reduction of RDX in the presence of magnetite.

The rate at which RDX is transformed by Fe^{II} adsorbed on magnetite may be described by the overall rate equation

$$-\mathrm{d[RDX]}/\mathrm{d}t = k_{ij}[\mathrm{Fe^{II}}]^{m}{}_{\mathrm{i}}[\mathrm{RDX}]_{j} \quad (1)$$

where *m* represents the apparent reaction order with respect to Fe^{II}, *i* represents different dissolved or adsorbed Fe^{II} species, *j* represents different dissolved or adsorbed RDX species, and k_{ij} is the rate coefficient for the reaction of species *i* and *j*. A similar formulation has been used to describe the reaction of oxamyl with Fe^{II} species (*40*). We observed little sorption of RDX onto magnetite, and for pH below 8.0, we observed negligible transformation of RDX by aqueous Fe^{II}, leading to the simplified rate expression

$$-\mathrm{d[RDX]}/\mathrm{d}t = k_{\mathrm{Fe^{II}}}[\mathrm{Fe^{II}}]^{m}{}_{\mathrm{ads,i}}[\mathrm{RDX}] \quad (2)$$

Under conditions of excess Fe^{II}, a pseudo-first-order rate coefficient (k_{obs}) for RDX transformation (equal to $k_{Fe^{II}}[Fe^{II}]^{m}{}_{ads,i}$) will be observed.

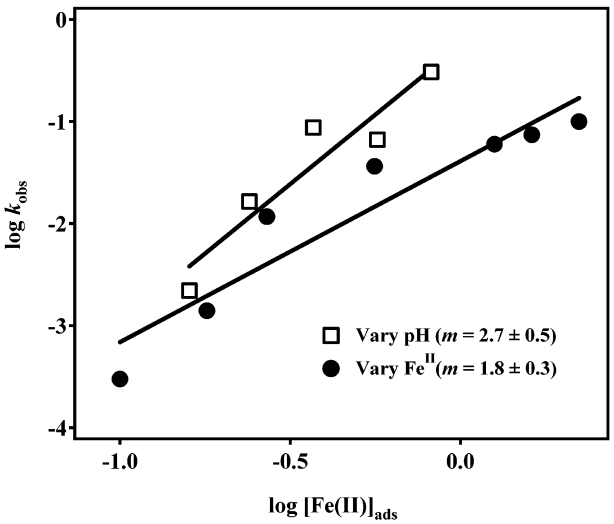

FIGURE 4. Apparent reaction order plot for RDX transformation by Fe^{II} adsorbed on magnetite. Lines are linear regressions of two data sets (●) varying initial $[Fe^{II}]_{dis}$ and (□) varying pH.

Values of k_{obs} estimated from Figure 3 increase as the amount of adsorbed Fe^{II} increases (Table 1). This is consistent with previous observations of transformation of nitroaromatic compounds (*25*), carbon tetrachloride (*29*), and dichlorodibromomethane (*30*). A plot of log k_{obs} vs log $[Fe^{II}]_{ads}$ indicates an apparent reaction order with respect to total adsorbed Fe^{II}, *m*, equal to 1.8 ± 0.3 (Figure 4). Others have reported fractional-order dependence (*61*), first-order dependence (*42*), and second-order dependence (*29*) on adsorbed Fe^{II} concentration for reduction of chromate, oxamyl, and carbon tetrachloride, respectively. Fendorf and Li (*61*) attributed the fractional dependence to a multi-step reaction by which Cr^{VI} was reduced to Cr^{III}. Amonette et al. (*29*) proposed a termolecular elementary reaction to explain their kinetic analyses in which an apparent reaction order of 1.97 was reported. On the basis of the data presented here, it would appear that the transformation of RDX is approximately second order with respect to adsorbed Fe^{II} concentration. Data for a range of observed dependences of k_{obs} on adsorbed Fe^{II} for a variety of target compounds are presented in the Supporting Information (Figure S1).

Effect of pH on Fe^{II} Adsorption and RDX Transformation Rates. For a constant initial dissolved Fe^{II} concentration of 1.6 mM, raising the solution pH resulted in faster rates of RDX transformation (Figure 5). Slow RDX transformation was observed at pH 6.0. As pH was increased, RDX was removed more rapidly. The faster rates observed at higher pH are most likely due to the greater amounts of Fe^{II} adsorbed at higher pH values as shown in Figure 6. A plot of $[Fe^{II}]_{ads}$ and k_{obs} values for RDX transformation (estimated from Figure 5) as a function of pH shows distinctly similar trends. As pH increases, more Fe^{II} adsorbs and k_{obs} increases, consistent with previous studies (*25*, *28*−*31*, *41*). Duplicate data sets at pH 7.0 (in Figures 5 and 6) indicate duplicate experiments performed in 50 mM MOPS and 50 mM HEPES buffered systems to determine whether there was a buffer effect on Fe^{II} adsorption or k_{obs}. As may be seen in Figure 6 and Table 1, about 30% less Fe^{II} was adsorbed to the surface in HEPES buffer than in MOPS buffer, though the statistical significance of this difference was not tested. Interestingly, k_{obs} was relatively unaffected, suggesting that the amount of Fe^{II} adsorbed is not the only factor affecting the rate of RDX transformation. Similar buffer effects with "Good's" buffers have been reported (*62*, *63*) and may be attributed to metal

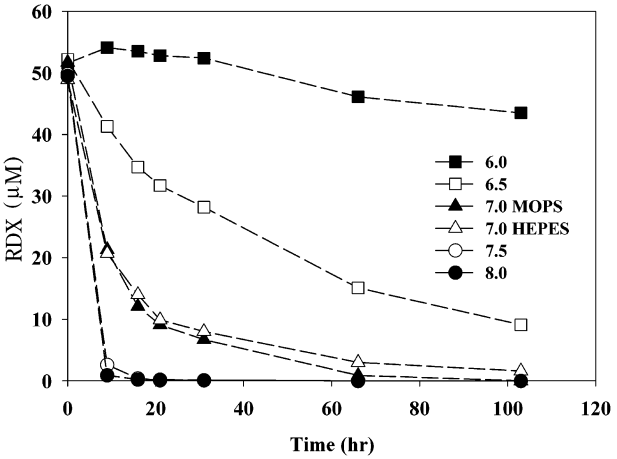

FIGURE 5. Transformation of RDX by an initial concentration of 1.6 mM $[Fe^{II}]_{dis}$ on 44 m^2 L^{-1} magnetite at various pH values.

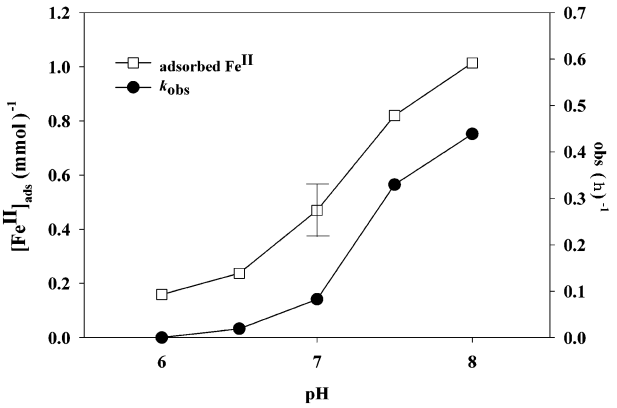

FIGURE 6. Adsorption of 1.6 mM Fe^{II} on 44m^2 L^{-1} magnetite and k_{obs} for removal of RDX as a function of pH. The two markers at pH 7.0 indicate separate MOPS and HEPES buffered systems.

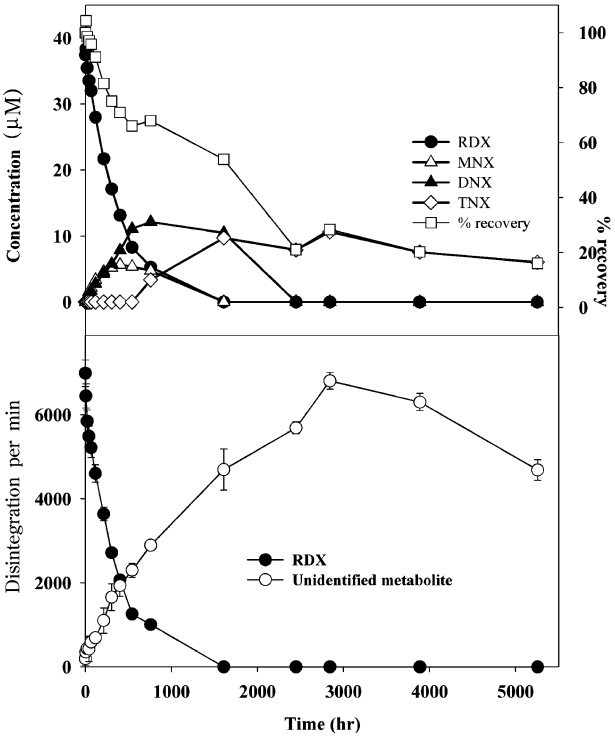

FIGURE 7. (Top) Disappearance of RDX and transient formation of MNX, DNX, and TNX. The reactor contained 44 m^2 L^{-1} magnetite and 0.15 mM $[Fe^{II}]_{ads}$ in 50 mM, pH 7.0 MOPS buffer. (Bottom) Transformation of [^{14}C]RDX by adsorbed Fe^{II} on magnetite under conditions similar to those described above. The figure shows production of an early-arriving transformation product observed on RCD chromatograms.

complexation (*64*). Referring to Figure 6, as the pH was increased from 6.0 to 8.0, $[Fe^{II}]_{ads}$ increased consistent with what would be expected for cation adsorption (as a result of less competition from H^+ adsorption at higher pH values). Based on Figure 6, a zero point of charge (ZPC) of between 7.0 and 7.5 can be estimated. Others have reported a ZPC for magnetite of 6.5 (*45*). A similar pH dependence for Fe^{II} adsorption on oxides has been observed in numerous previous studies (*25*, *28*−*31*, *40*, *57*, *65*−*67*). Others have suggested that the pH dependence of Fe^{II} adsorption to oxide surfaces may also be indicative of the formation of different surface species (*25*, *28*−*30*, *39*, *65*).

To decouple the effect of pH and amount of Fe^{II} adsorbed on k_{obs}, we compared the two sets of data obtained from experiments in which (i) the initial $[Fe^{II}]_{dis}$ was varied at constant pH 7.0 and (ii) pH was varied at constant initial $[Fe^{II}]_{dis}$ (Figure 4). If the increases in k_{obs} for the experiment in which pH was varied were due solely to deprotonation of the oxide surface and subsequent increase in $[Fe^{II}]_{ads}$, then the data sets would overlap and have similar slopes (as was observed for oxamyl transformation by Fe^{II} (*40*)). Varying the pH results in a slope of 2.7 ± 0.5, whereas varying the amount of Fe^{II} results in a slope of 1.8 ± 0.3 (Figure 4). Linear regression of the entire data set results in a slope of 1.7 ± 0.4. Though the slopes for the two separate data sets are similar, a slight divergence is observed at higher pH values, suggesting that increases in k_{obs} may not be solely the result of increased Fe^{II} adsorption, but may also be influenced by the formation of different surface species of greater reactivity at higher pH. This dependence on solution pH also alludes to a surface reaction in which Fe^{II} complexes of differing reactivity are responsible for the transformation of RDX (*25*, *28*, *30*, *65*) and is consistent with the postulate by Liger et al. (*28*) that the hydrolytic surface complexes $\equiv Fe^{III}OFe^{II}OH^0$, which are predominantly formed at pH > 7.0 (*39*), may be a better reductant than the complex $(\equiv Fe^{III}OFe^{II})^+$.

To determine the apparent reaction order with respect to pH, initial $[Fe^{II}]_{dis}$ was held constant while pH was varied. A plot of log k_{obs} vs pH and linear regression of the data (not shown) for pH 6.5, 7.0, and 7.5 gave an apparent reaction order of 1.3 ± 0.1 (Figure S2 in the Supporting Information). The value of k_{obs} at pH 8.0 did not fit well with the other three points, further suggesting that precipitation may have contributed to the measured Fe^{II} losses from solution. As discussed above, in the absence of magnetite, Fe^{II} precipitated and partially transformed RDX at pH 8.0. Others have reported similar apparent reaction orders with respect to pH for transformation of organic contaminants by adsorbed Fe^{II} (*25*, *29*, *30*).

Products of RDX Transformation. The transformation of RDX in the presence of Fe^{II} and magnetite resulted in the production of the three sequential nitro reduction products MNX, DNX, and TNX (Figure 7). As 40 μM RDX was transformed, a concomitant production of MNX and DNX was observed. MNX was detected as high as 5 μM and DNX as high as 12 μM. Both MNX and DNX were produced transiently, with MNX concentrations decreasing after 500 h of reaction. Since MNX and DNX were formed simultaneously, it is not clear from the data whether DNX arose directly from RDX or was a product of MNX reduction. TNX concentrations reached a maximum of 10 μM after about 1000 h of reaction and, though diminishing, persisted for at least 5000 h. However, after a year of reaction, TNX was not detected. After RDX was below its detection limit (~1600 h),

the sum of the nitroso derivatives accounted for no more than 60% of the initial RDX on a molar basis (Figure 7). The sum of MNX, DNX, and TNX decreased until approximately 4000 h of reaction, when the sum of these products represented less that 20% of the initial RDX.

The lack of a mass balance with respect to nitroso intermediates indicated that other product(s) were formed. The headspace of reactors was sampled for GC analysis of nitrous oxide on two occasions (1500 and 3800 h). Though others have found that N_2O is an end product of biological transformation (*35*, *52*), anaerobic sludge-augmented Fe^0 treatment (*35*), and alkaline hydrolysis (*68*) of RDX, N_2O was not observed above its detection limit of approximately 2 μM at either sampling time in our reactors. Liquid samples were taken for IC analysis of ammonium and nitrite after 3800 h and a year of incubation. Nitrite was not detected. This negative result, however, does not necessarily indicate that denitration did not occur since nitrite is known to react with adsorbed Fe^{II} (*69*). After 3800 h, NH_4^+ was found to have accumulated to 39 μM in these reactors, which accounts for approximately 17% of the total N available from RDX. Similar quantities of NH_4^+ have been observed for the treatment of RDX-contaminated soil with Fe^0 (*6*, *7*). In these nonsterile studies with soil, from 17.5% (*6*) to 50% (*7*) of the total RDX N was recovered as NH_4^+. Singh et al. (1998) attribute much of the remaining RDX N to C−N products, but concede that headspace loss of NH_3 was possible, as well as losses from other gaseous N species. However, in our reactors at pH 7.0, significant equilibrium partitioning of NH_3 ($pK_a = 9.3$) would not be expected. It is possible that RDX may undergo alkaline hydrolysis to produce other gaseous products such as N_2O and N_2 (*68*, *70*, *71*); however, we did not observe hydrolysis of RDX in buffered solutions at pH 7.0 (data not shown).

Parallel experiments with [^{14}C]RDX were conducted to help determine the ultimate fate of the carbon in RDX. Over the course of the experiment, an additional peak was seen to increase on UV and radiochemical detector (RCD) chromatograms (Figure 7, bottom). The peak arrived earlier than that of TNX, indicating that it was more polar TNX. The product accumulated in the aqueous phase and represented as much as 90% of the initial disintegrations per minute (DPM) from [^{14}C]RDX. Others have reported MEDINA, a C1 compound resulting from the hydrolysis of the RDX ring in biotic systems (*52*, *72*), nonsterile systems with Fe^0 (*8*), and treatment with Fenton's reagent (*73*). Under LC/MS conditions similar to those described previously (*8*, *52*) for the identification of MEDINA (and other transformation products), no significant mass shifts from [^{15}N]RDX, [^{13}C]RDX, and [^{12}C]RDX were observed. Mineralization was not a significant pathway for RDX transformation. Less than 10% was represented as $^{14}CO_2$. Though adsorption of RDX ring cleavage products to soil has been observed (*74*), extraction of magnetite solids with acetonitrile found that adsorption of radiolabel on mineral surfaces was not significant (<1%), as others have reported (*6*, *7*). Nor was radioactivity recovered from biological oxidation, indicating that covalently bound residues were not formed by RDX.

About one year later (10176 h), the unidentified ^{14}C peak was still present in the reactors, comprising about 70% of the total radioactivity. A portion of the ^{14}C peak was identified as formaldehyde using HPLC analysis and derivatization with DNPH. As shown in Figure 8, however, RCD chromatograms before and after DNPH derivitization result in only part of the peak shifting to the HCHO retention time. The unshifted portion of the peak indicates that there is still some unidentified, soluble product present. Quantification of formaldehyde revealed a concentration of 35 μM, which accounts for about 24% of the initial RDX carbon. Since the ultimate fate of all C and N from RDX was not determined, it is unclear whether ferrous iron reduction of RDX is a desirable mechanism of removal. However, it is well-known that reduced RDX products are more biodegradable than the parent compound.

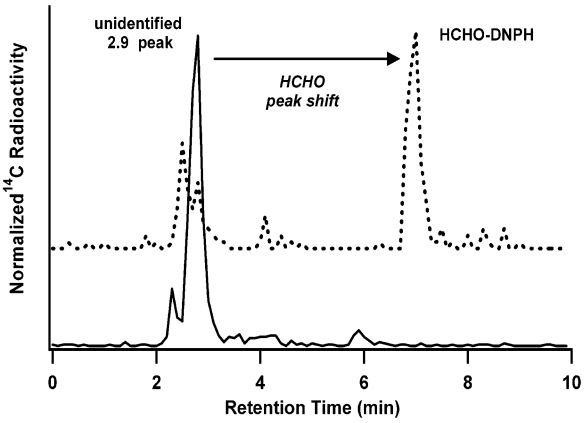

FIGURE 8. Partial shift in retention time for the early-arriving product observed on radiochemical detector chromatograms after derivatization with DNPH. Normalized peak signals are illustrated because differences in eluent chemistry resulted in different RCD signal intensities. The intensity for the formaldehyde derivitization sample is 10-fold lower than that for the initial sample.

Environmental Significance. RDX is a common subsurface contaminant at military installations and bomb-manufacturing facilities. Though transformations of RDX are well-known and iron is an abundant electron donor and acceptor, little is known about the transformation of RDX by iron species other than Fe^0. This study demonstrates that Fe^{II} bound to iron mineral may rapidly transform RDX. The rates of transformation are dependent on the amount of adsorbed Fe^{II}, suggesting that, in anoxic sediments or engineered environments where Fe^{II} is abundant, RDX transformation will be rapid. Furthermore, this study demonstrates that elevated pH values, such as those observed in Fe^0 permeable reactive barriers and some natural settings, favor the removal of RDX by adsorbed Fe^{II} species.

Acknowledgments

We thank Dr. Craig Just for his valuable assistance in developing analytical methods for this work. In addition, we thank Dr. Pedro Alvarez and Dr. Richard Valentine for helpful discussions. K.B.G. was supported by the National Science Foundation (NSF) Research Training Grant DBI9602247 and United States Public Health Service Training Grant 732 GM8365 through The University of Iowa Center for Biocatalysis and Bioprocessing. Additional support was provided by the NSF under Grant BES-9983719 and Strategic Environmental Research and Development Program (SERDP) Project DACA 72-00-P-0057.

Supporting Information Available

Figure S1 showing data used to estimate the range of reported dependencies of k_{obs} on adsorbed Fe^{II} under a variety of conditions and Figure S2 showing the data used to determine the dependency of k_{obs} for RDX transformation on pH. This material is available free of charge via the Internet at http://pubs.acs.org.

Literature Cited

(1) Haas, R.; Schreiber, I.; Low, E.; Stork, G. *Fresenius' J. Anal. Chem.* **1990**, *338*, 41−45.

(2) Byrd, J., Jr.; Humphreys, J. Department of Defense/Department of Energy (DOD/DOE) Research and Development (R&D) of Incineration Techniques for Demilitarization. Presented at the 12th International Incineration Conference, Knoxville, TN, May

3−7, 1993; *Proceedings of the International Incineration Conference*, Vol. 1-12; University of California: Irvine, 1993; pp 621−624.
(3) Robidoux, P. Y.; Svendsen, C.; Caumartin, J.; Hawari, J.; Ampleman, G.; Thiboutot, S.; Weeks, J. M.; Sunahara, G. I. *Environ. Toxicol. Chem.* **2000**, *19*, 1764−1773.
(4) Gong, P.; Hawari, J.; Thiboutot, S.; Ampleman, G.; Sunahara, G. I. *Environ. Toxicol. Chem.* **2001**, *20*, 947−951.
(5) Yinon, J.; Zitrin, S. *Modern Methods and Applications in the Analysis of Explosives*; John Wiley & Sons Ltd.: West Sussex, England, 1993.
(6) Singh, J.; Comfort, S. D.; Shea, P. J. *J. Environ. Qual.* **1998**, *27*, 1240−1245.
(7) Hundal, L. S.; Singh, J.; Bier, E. L.; Shea, P. J.; Comfort, S. D.; Powers, W. L. *Environ. Pollut.* **1997**, *97*, 55−64.
(8) Oh, B.-T.; Just, C. L.; Alvarez, P. J. J. *Environ. Sci. Technol.* **2001**, *35*, 4341−4346.
(9) U.S. Environmental Protection Agency. *Long-term performance of permeable reactive barriers using zero-valent iron: an evaluation of two sites*; EPA: Washington, DC, 2002.
(10) Phillips, D. H.; Gu, B.; Watson, D. B.; Roh, Y.; Liang, L.; Lee, S. Y. *Environ. Sci. Technol.* **2000**, *34*, 4196−4176.
(11) Farrel, J.; Kason, M.; Melitas, N.; Li, T. *Environ. Sci. Technol.* **2000**, *34*, 514−521.
(12) Klausen, J.; Ranke, J.; Schwarzenbach, R. P. *Chemosphere* **2001**, *44*, 511−517.
(13) Yabusaki, S.; Cantrell, K.; Sass, B.; Steefel, C. *Environ. Sci. Technol.* **2001**, *35*, 1493−1503.
(14) Ritter, K.; Odziemkowski, M. S.; Gillham, R. W. *J. Contam. Hydrol.* **2002**, *55*, 87−111.
(15) Gu, B.; Phelps, T., J.; Liang, L.; Dickey, M., J.; Roh, Y.; Kinsall, B., L.; Palumbo, A., V.; Jacobs, G. K *Environ. Sci. Technol.* **1999**, *33*, 2170−2177.
(16) Pratt, A. R.; Blowes, D. W.; Ptacek, C. J. *Environ. Sci. Technol.* **1997**, *31*, 2492−2498.
(17) Peterson, M.; Brown, G.; Parks, G.; Stein, C. *Geochim. Cosmochim. Acta* **1997**, *61*, 3392−3412.
(18) Vogan, J.; Focht, R.; Clark, D.; Graham, S. *J. Hazard. Mater.* **1999**, *68*, 97−108.
(19) Scherer, M. M.; Balko, B. A.; Tratnyek, P. G. In *Mineral-Water Interfacial Reactions: Kinetics and Mechanisms*; Grundl, T., Ed.; American Chemical Society: Washington, DC, 1999.
(20) Haderlein, S. B.; Pecher, K. In *Mineral-Water Interfacial Reactions: Kinetics and Mechanisms*; Grundl, T., Sparks, D., Eds.; ACS Symposium Series 715; American Chemical Society: Washington, DC, 1998; pp 342−357.
(21) Amonette, J. E. C. (Clay Minerals Society). In *Electrochemistry of Clays*; Fitch, A., Ed.; Clay Minerals Society: Aurora, CO, 2002; Vol. 10.
(22) Patterson, R., R; Fendorf, S.; Fendorf, M. *Environ. Sci. Technol.* **1997**, *31*, 2039−2044.
(23) Butler, E. C.; Hayes, K. F. *Environ. Sci. Technol.* **1998**, *32*, 1276−1284.
(24) Williams, A. G. B.; Scherer, M. M. *Environ. Sci. Technol.* **2001**, *35*, 3488−3494.
(25) Klausen, J.; Trober, S. P.; Haderlein, S. B.; Schwarzenbach, R. P. *Environ. Sci. Technol.* **1995**, *29*, 2396−2404.
(26) Cui, D.; Eriksen, T. E. *Environ. Sci. Technol.* **1996**, *30*, 2259−2262.
(27) Buerge, I. J.; Hug, S. J. *Environ. Sci. Technol.* **1999**, *33*, 4285−4291.
(28) Liger, E.; Charlet, L.; Van Cappellen, P. *Geochim. Cosmochim. Acta* **1999**, *63*, 2939−2955.
(29) Amonette, J. E.; Workman, D. J.; Kennedy, D. W.; Fruchter, J. S.; Gorby, Y. A. *Environ. Sci. Technol.* **2000**, *34*, 4606−4613.
(30) Pecher, K.; Haderlein, S. B.; Schwarzenbach, R. P. *Environ. Sci. Technol.* **2002**, *36*, 1734−1741.
(31) Vikesland, P. J.; Valentine, R. L. *Environ. Sci. Technol.* **2002**, *36*, 512−519.
(32) Hering, J. G.; Stumm, W. In *Reviews in Mineralogy*; Ribbe, P. H., Ed.; Mineralogical Society of America: Washington, DC, 1990; pp 427−465.
(33) Smolen, J. M. *Aquat. Sci.*, in press.
(34) McCormick, M. L.; Bouwer, E. J.; Adriaens, P. *Environ. Sci. Technol.* **2002**, *36*, 403−410.
(35) Gregory, K. B.; Von Arb, M.; Alvarez, P. J. J.; Scherer, M. M.; Parkin, G. F. In *Bioremediation of Energetics, Phenolics, and Polycyclic Aromatic Hydrocarbons*; Magar, V. S., Johnson, G., Ong, S. K., Leeson, A., Eds.; Battelle Press: Colombus, OH, 2001; pp 1−9.
(36) Lloyd, J. R.; Sole, V. A.; Van Praagh, C. V. G.; Lovley, D. R. *Appl. Environ. Microbiol.* **2000**, *66*, 3743−3749.
(37) Hofstetter, T. B.; Heijman, C. G.; Haderlein, S. B.; Holliger, C.; Schwarzenbach, R. P. *Environ. Sci. Technol.* **1999**, *33*, 1479−1487.
(38) Heijman, C., G.; Grieder, E.; Holliger, C.; Schwarzenbach, R. P *Environ. Sci. Technol.* **1995**, *29*, 775−783.
(39) Charlet, L.; Silvester, E.; Liger, E. *Chem. Geol.* **1998**, *151*, 85−93.
(40) Strathmann, T. J.; Stone, A. T. *Geochim. Cosmochim. Acta*, in press.
(41) Klupinski, T. P.; Chin, Y.-P. *Environ. Sci. Technol.* **2003**, *37*, 1311−1318.
(42) Strathmann, T. J.; Stone, A. T. *Environ. Sci. Technol.* **2002**, *36*, 5172−5183.
(43) Strathmann, T. J.; Stone, A. T. *Environ. Sci. Technol.* **2002**, *36*, 653−661.
(44) Buerge, I. J.; Hug, S. J. *Environ. Sci. Technol.* **1998**, *32*, 2092−2099.
(45) Stumm, W. In *Chemistry of the Solid-Water Interface* Stumm, W., Ed.; John Wiley & Sons: New York, 1992.
(46) Beller, H. R.; Tiemeier, K. *Environ. Sci. Technol.* **2002**, *36*, 2060−2066.
(47) Lovley, D. R.; Reynolds, R. L. *Eos* **1987**, *68*, 1258.
(48) Zachara, J. M.; Kukkadapu, R. K.; Fredirickson, J. K.; Gorby, Y. A.; Smith, S. C. *Geomicrobiol. J.* **2002**, *19*, 179−207.
(49) Ampleman, G.; Thiboutot, S.; Lavigne, J.; Marois, A.; Hawari, J.; Jones, A. M.; Rho, D. *J. Labelled Compd. Radiopharm.* **1995**, *36*, 559−577.
(50) Good, N. E.; Winget, D. C.; Winter, W.; Connolly, T. N.; Izawa, S.; Singh, R. M. M. *Biochemistry* **1966**, *5*, 467−477.
(51) Good, N. E.; Izawa, S. *Methods Enzymol.* **1972**, *24*, 53−68.
(52) Hawari, J.; Halasz, A.; Sheremata, T. W.; Beaudet, S.; Groom, C.; Paquet, L.; Rhofir, C.; Ampleman, G.; Thiboutot, S. *Appl. Environ. Microbiol.* **2000**, *66*, 2652−2657.
(53) *Civil and Environmental Engineering*; The University of Iowa: Iowa City, 2001.
(54) Stookey, L. L. *Anal. Chem.* **1970**, *42*, 779−781.
(55) Lovley, D., R.; Phillips, E. J. P. *Appl. Environ. Microbiol.* **1986**, *52*, 751−757.
(56) Wehrli, B. In *Aquatic Chemical Kinetics: Reaction Rates of Processes in Natural Waters* Stumm, W., Ed.; Wiley-Interscience: New York, 1990; pp 311−336.
(57) Jeon, B.-H.; Dempsey, B. A.; Burgos, W. D.; Royer, R. A. *Colloids Surf., A* **2001**, *191*, 41−55.
(58) Farley, K. J.; Dzombak, D. A.; Morel, F. M. M. *J. Colloid Interface Sci.* **1985**, *106*, 226−242.
(59) Dzombak, D. A.; Morel, F. M. M. *Surface Complexation Modeling: Hydrous Ferric Oxide*; John Wiley and Sons: New York, 1990.
(60) Waychunas, G.; Davis, J.; Reitmeyer, R. *J. Synchrotron Radiat.* **1999**, *6*, 615−617.
(61) Fendorf, S. E.; Li, G. *Environ. Sci. Technol.* **1996**, *30*, 1614−1617.
(62) Alowitz, M. J.; Scherer, M. M. *Environ. Sci. Technol.* **2002**, *36*, 299−306.
(63) Nakon, R.; Krishnamoorthy, C. R. *Science* **1983**, *221*, 749−750.
(64) Mash, H. E.; Chin, Y.-P. *Anal. Chem.* **2003**, *75*, 671−677.
(65) Zhang, Y. L.; Charlet, L.; Schindler, P. W. *Colloids Surf.* **1992**, *63*, 259−268.
(66) Liger, E.; Charlet, L.; Spadini, L.; Lovgren, L. *J. Colloid Interface Sci.* **1997**.
(67) Schultz, C. A.; Grundl, T. J. *Environ. Sci. Technol.* **2000**, *34*, 3641−3648.
(68) Heilmann, H. M.; Wiesmann, U.; Senstrom, M. K. *Environ. Sci. Technol.* **1996**, *30*, 1485−1492.
(69) Sorenson, J.; Thorling, L. *Geochim. Cosmochim. Acta* **1991**, *55*, 1289−1294.
(70) Hoffsommer, J. C.; Kubose, D. A.; Glover, D. J. *J. Phys. Chem.* **1977**, *81*, 380−385.
(71) Croce, M.; Okamoto, Y. *J. Org. Chem.* **1979**, *44*, 2100−2103.
(72) Halasz, A.; Spain, J.; Paquet, L.; Beaulieu, C.; Hawari, J. *Environ. Sci. Technol.* **2002**, *36*, 633−638.
(73) Bier, E. L.; Singh, J.; Li, Z.; Comfort, S. D.; Shea, P. J. *Environ. Toxicol. Chem.* **1999**, *18*, 1078−1084.
(74) Sheremata, T. W.; Halasz, A.; Paquet, L.; Thiboutot, S.; Ampleman, G.; Hawari, J. *Environ. Sci. Technol.* **2001**, *35*, 1037−1040.

Received for review June 11, 2003. Revised manuscript received November 10, 2003. Accepted November 15, 2003.

ES034588W